Behavior of a Pentacle Connected Five-Phase IM Supplied by a Rectangular Voltage

Pavel ZASKALICKY

Department of Electrical Engineering and Mechatronics, Faculty of Electrical Engineering and Informatics, Technical University of Kosice, Letna 9, 042 00 Kosice, Slovak Republic

pavel.zaskalicky@tuke.sk

DOI: 10.15598/aeee.v18i2.3430

Abstract. *The presented article deals with the steady-state analysis of five-phase Induction Motor (IM), which is supplied by rectangular voltage from a five-leg Voltage Source Inverter (VSI). The new proposed approach is derived from complex Fourier-series using to express inverter terminal voltages. Based on mathematically described inverter output voltages, a formula for VSI output space phasor was derived. Assuming sinusoidal motor winding distribution and on the basis of motor parameters, stator and rotor current space phasors for defined motor load were determined. Finally, the electromagnetic torque ripple waveforms for different IM operation states were investigated.*

Keywords

Complex Fourier series, five-phase inverter, induction machine, torque ripple, rectangular voltage.

1. Introduction

Variable speed electric drives, in general, preferentially utilize three-phase induction machines. Providing that the variable speed Alternating Current (AC) drives require a power electronic converter, the number of machine phases is practically unlimited. This fact led to an increasing interest for multiphase AC drives applications. Most often, they are five-phase induction machines that, by their nature, offer some advantages over their three-phase counterparts.

E. E. Ward and Harrer [1], for the first time in 1969, have presented the preliminary investigation on inverter fed five-phase IM and suggested that the amplitude of torque pulsation could be reduced by increasing the number of phases [2].

Major advantages of using a five-phase machine instead of the three-phase one consist of its higher torque density, greater efficiency and fault tolerance [3], [4] and [5]. Other advantages include reduced electromagnetic torque pulsation and reduction in the required rating per inverter leg. Noise characteristics of the five-phase drives are better when compared with the three-phase ones. For this reason, it is expected to use them in residential areas and hospitals where noise presents an undesirable element.

In the majority of cases, the supply for a multiphase variable-speed AC drives is provided by a Voltage Source Inverter (VSI) [6]. Output voltage control has a significant effect on the electromagnetic torque ripple of the motor. Control of VSI is provided in prevail by Pulse Width Modulation (PWM) techniques. Space Vector PWM (SVPWM) has become the most popular because of its easy digital implementation. However, some industrial applications of the five-phase drives do not need to modulate the output voltage. Because the rectangular voltage supply causes the ripple in motor's electromagnetic torque, the inverter control is easier and reduces requirements on semiconductor switching units [7], [8], [9] and [10].

2. Modeling of a Five-Phase VSI

The power circuit topology of a five-phase source inverter is shown in Fig. 1. VSI consists of a parallel connection of five transistor legs denoted $(a, b, \ldots, e)$. It is supplied by a constant voltage source provided by an isolated Direct Current (DC)-source and a capacitive DC-link. Each leg is composed of two Insulated-

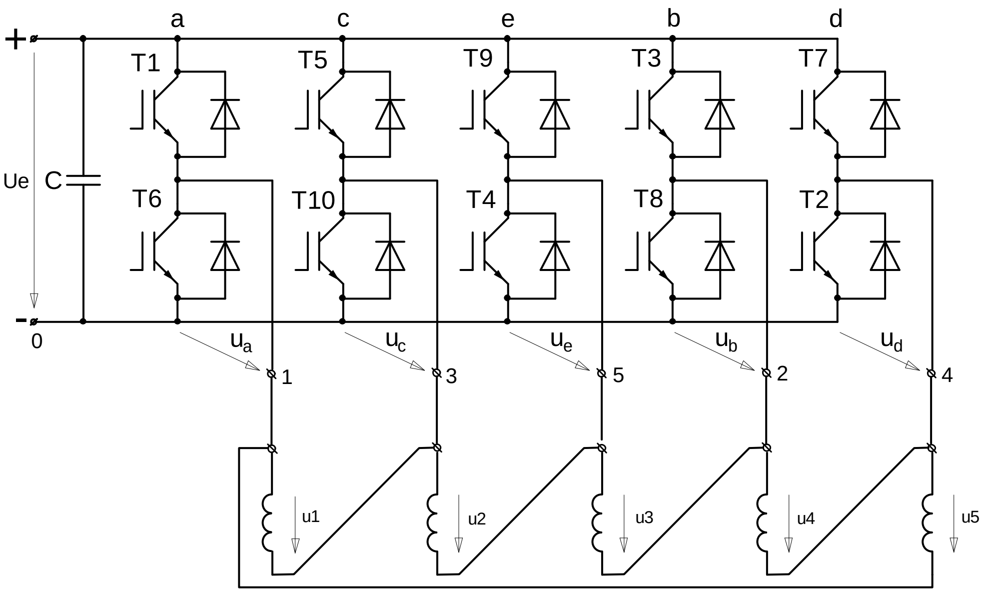

Fig. 1: Five-phase bridge connected VSI.

Gate Bipolar Transistor (IGBT) transistors with anti-parallel connected free-wheeling diodes used to ensure a negative current path through the switches. Inverters output terminals are numbered $(1, 2, \ldots, 5)$ [11].

To build a mathematical model of VSI, the complex Fourier series were used. They are extremely useful as a way to break up an arbitrary periodic function into a set of simple terms that can be solved individually and then recombined to obtain the solution to the original problem.

In the next, we assume idealized semiconductor devices which satisfy the following properties:

- Power switches can handle unlimited current, and they are able to block unlimited voltage.
- Voltage drop across the switch and leakage current are zero.
- The switches are turned on and off with no rise and fall times.
- Inverter input capacity is sufficiently high so we can suppose the converter input DC voltage constant for any output currents.

These assumptions simplify analysis of the power circuit and help to build against mathematical model.

The transistors in each leg are switched so that they form voltage impulses over the half period of the desired output frequency. The voltage impulse of the first transistors leg measured against the negative pole of the DC link can be expressed as [12], [13] and [14]:

$$\mathbf{u}_a = \mathbf{u}_{dc} + \mathbf{u}_{01} = \frac{U_e}{2} + 2\,U_e\,\mathsf{Re}\left(\sum_{k=1}^{\infty} c_k\, e^{jk\omega t}\right), \quad (1)$$

where $\mathbf{u}_{dc}$ is DC and $\mathbf{u}_{01}$ is AC voltage component, U_e is DC link voltage and c_k is Fourier coefficient defined as:

$$c_k = \frac{1}{j2k\pi}\left(1 - e^{-jk\pi}\right) \quad \text{valid for } k \neq 0. \quad (2)$$

Figure 2 shows the first leg output voltage waveform calculated on the base of Eq. (1). This was drawn for DC supply $U_e = 350\,\mathrm{V}$ and output frequency $f = 50\,\mathrm{Hz}$.

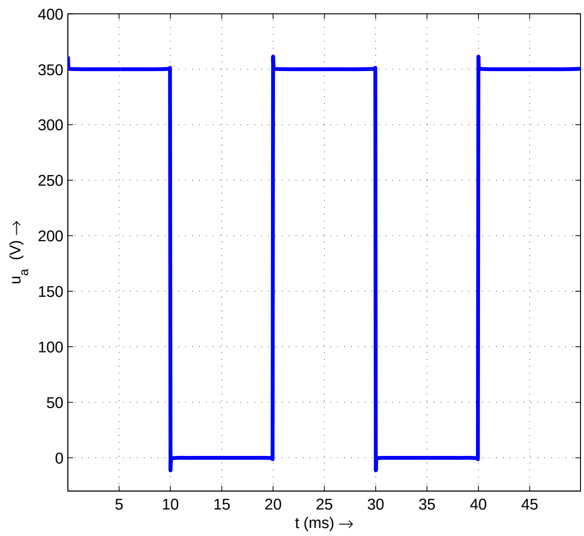

Fig. 2: Inverter leg voltage waveform.

Voltages of the other legs are mutually displaced by the voltage shifting factor $\mathbf{a} = e^{j\frac{2k\pi}{5}}$. Then, we can express them as:

$$\begin{aligned} \mathbf{u}_b &= \mathbf{a}\mathbf{u}_a, & \mathbf{u}_c &= \mathbf{a}^2\mathbf{u}_a, \\ \mathbf{u}_d &= \mathbf{a}^3\mathbf{u}_a, & \mathbf{u}_e &= \mathbf{a}^4\mathbf{u}_a. \end{aligned} \tag{3}$$

Motor phase voltages are given by the difference of voltages between two legs. Since $\mathbf{a}\,\mathbf{u}_{dc} = \mathbf{a}^2\mathbf{u}_{dc} = \mathbf{a}^3\mathbf{u}_{dc} = \mathbf{a}^4\mathbf{u}_{dc} = \mathbf{u}_{dc}$ (DC voltage shift), the phase voltages can be expressed as follows:

$$\begin{aligned} \mathbf{u}_1 &= \mathbf{u}_a - \mathbf{u}_c = (1-\mathbf{a}^2)\mathbf{u}_{01}, \\ \mathbf{u}_2 &= \mathbf{u}_c - \mathbf{u}_e = (\mathbf{a}^2-\mathbf{a}^4)\mathbf{u}_{01}, \\ \mathbf{u}_3 &= \mathbf{u}_e - \mathbf{u}_b = (\mathbf{a}^4-\mathbf{a})\mathbf{u}_{01}, \\ \mathbf{u}_4 &= \mathbf{u}_b - \mathbf{u}_d = (\mathbf{a}-\mathbf{a}^3)\mathbf{u}_{01}, \\ \mathbf{u}_5 &= \mathbf{u}_d - \mathbf{u}_a = (\mathbf{a}^3-1)\mathbf{u}_{01}, \end{aligned} \tag{4}$$

where $\mathbf{u}_{01} = 2\,U_e\,\mathrm{Re}\left(\sum_{k=1}^{\infty} c_k\, e^{jk\omega t}\right)$ is the AC component of the voltage $\mathbf{u}_a$.

Figure 3 shows a phasor diagram of the pentacle connected five-phase voltage system. The phase voltages are mutually shifted by $2\,\frac{2\pi}{5}$. These form a second-order voltage system.

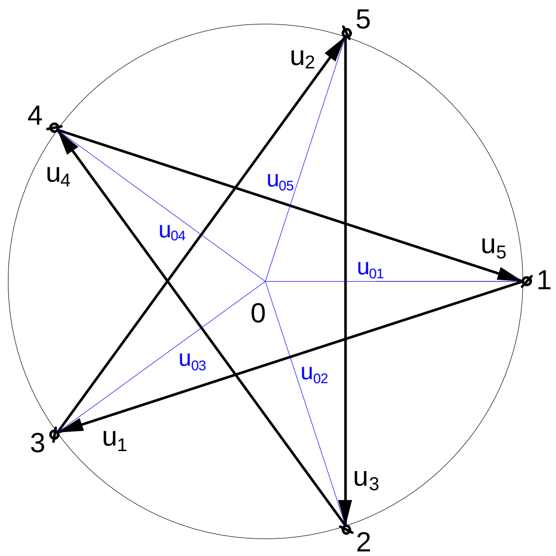

Fig. 3: Phasor diagram of the pentacle connected five phase voltage system.

Figure 4 depicts the motor phase voltage waveform calculated on the base of Eq. (1) and Eq. (4).

To simplify the calculation of AC motor quantities, it is advantageous to employ space phasors. This transformation is very often used for the analysis of multi-phase electric systems. The term "space" originally stands for the two-dimensional complex plane, in which the multi-phase quantities are transformed.

The transformation of space phasor is directly derived from the sum of voltage phase phasors. Based on the Eq. (4), the space phasor transformation is thus defined as published in [15], [16] and [17]:

$$\underline{\mathbf{u}} = \frac{2}{5}\Big[\mathrm{Re}(\mathbf{u}_1) + \mathrm{Re}(\mathbf{u}_2)\mathbf{a}_1 + \mathrm{Re}(\mathbf{u}_3)\mathbf{a}_1^2 + +\mathrm{Re}(\mathbf{u}_4)\mathbf{a}_1^3 + \mathrm{Re}(\mathbf{u}_5)\mathbf{a}_1^4\Big], \tag{5}$$

where $\mathbf{a}_1 = e^{j2\frac{2\pi}{5}}$ is the space shifting factor for the second-order system.

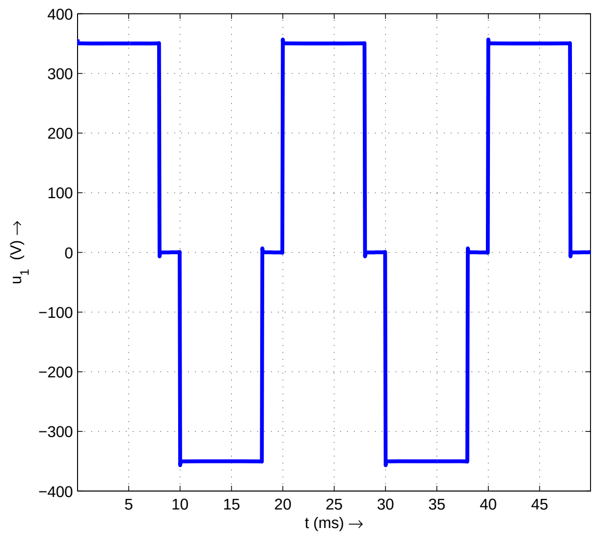

Fig. 4: Motor phase voltage waveform.

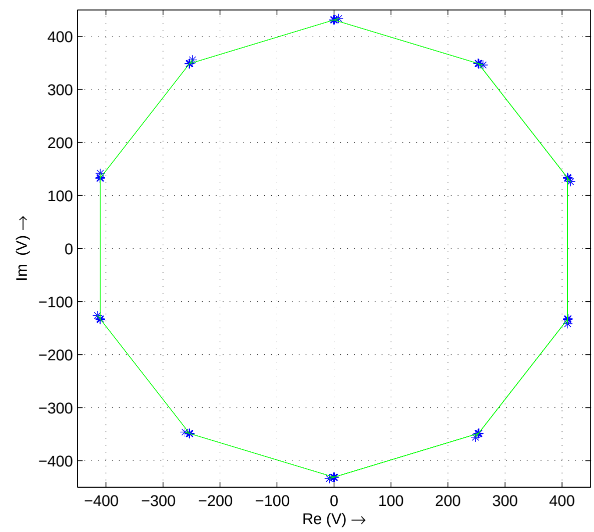

Fig. 5: Voltage space phasor trajectory.

Coefficient $\frac{2}{5}$ keeps the magnitude of the phasors during the transformation constant.

In the Fig. 5, there is shown the VSI output voltage space phasor trajectory. The green lines represent the path of voltage space phasor jump.

The real and imaginary parts of the voltage space phasor can be separated and rewritten as:

$$\mathbf{u} = \mathsf{Re}(\underline{\mathbf{u}}) + \mathsf{Im}(\underline{\mathbf{u}}) = u_\alpha + u_\beta. \tag{6}$$

By using space phasor, the multi-phase components are transformed into a two-dimensional coordinate system. They are shown in Fig. 6.

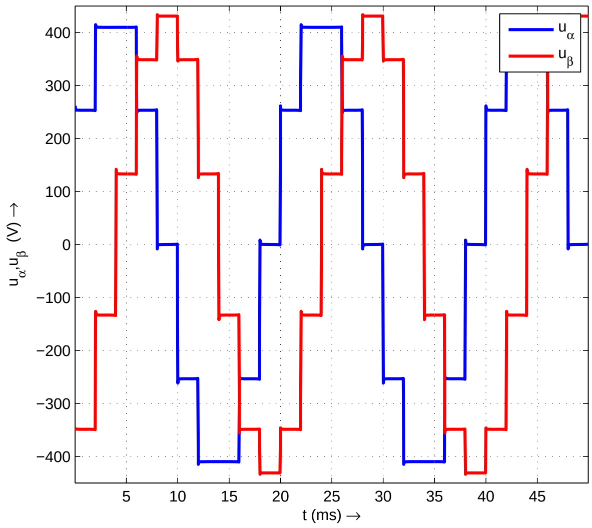

Fig. 6: Two-dimensional voltage system components.

For further calculations, it is necessary to perform harmonic analysis of the two-phase voltage system. The following equations apply to the amplitudes of two-phase voltage harmonic components $A_{\alpha k}$ and $A_{\beta k}$, where $k = 1, 2, 3, \ldots$:

$$\begin{aligned} A_{\alpha k} &= \frac{2}{5}\,\mathsf{abs}\Big[\mathsf{Re}(\mathbf{u}_1) + \mathsf{Re}(\mathbf{u}_2)\mathbf{a}_1 + \mathsf{Re}(\mathbf{u}_3)\mathbf{a}_1^2 + \\ &\quad + \mathsf{Re}(\mathbf{u}_4)\mathbf{a}_1^3 + \mathsf{Re}(\mathbf{u}_5)\mathbf{a}_1^4\Big], \\ A_{\beta k} &= \frac{2}{5}\,\mathsf{abs}\Big[\mathsf{Im}(\mathbf{u}_1) + \mathsf{Im}(\mathbf{u}_2)\mathbf{a}_1 + \mathsf{Im}(\mathbf{u}_3)\mathbf{a}_1^2 + \\ &\quad + \mathsf{Im}(\mathbf{u}_4)\mathbf{a}_1^3 + \mathsf{Im}(\mathbf{u}_5)\mathbf{a}_1^4\Big]. \end{aligned} \tag{7}$$

For each phase of harmonics, the phase shift is calculated as follows:

$$\begin{aligned} \phi_{\alpha k} &= \mathsf{arg}\Big[\mathsf{Re}(\mathbf{u}_1) + \mathsf{Re}(\mathbf{u}_2)\mathbf{a}_1 + \mathsf{Re}(\mathbf{u}_3)\mathbf{a}_1^2 + \\ &\quad + \mathsf{Re}(\mathbf{u}_4)\mathbf{a}_1^3 + \mathsf{Re}(\mathbf{u}_5)\mathbf{a}_1^4\Big], \\ \phi_{\beta k} &= \mathsf{arg}\Big[\mathsf{Im}(\mathbf{u}_1) + \mathsf{Im}(\mathbf{u}_2)\mathbf{a}_1 + \mathsf{Im}(\mathbf{u}_3)\mathbf{a}_1^2 + \\ &\quad + \mathsf{Im}(\mathbf{u}_4)\mathbf{a}_1^3 + \mathsf{Im}(\mathbf{u}_5)\mathbf{a}_1^4\Big]. \end{aligned} \tag{8}$$

Figure 7 depicts calculated harmonic components of the two-phase voltages. Voltage waveforms are composed of $1, 9, 11, 19, 21, 29, 31, \ldots$ harmonics. Waves of

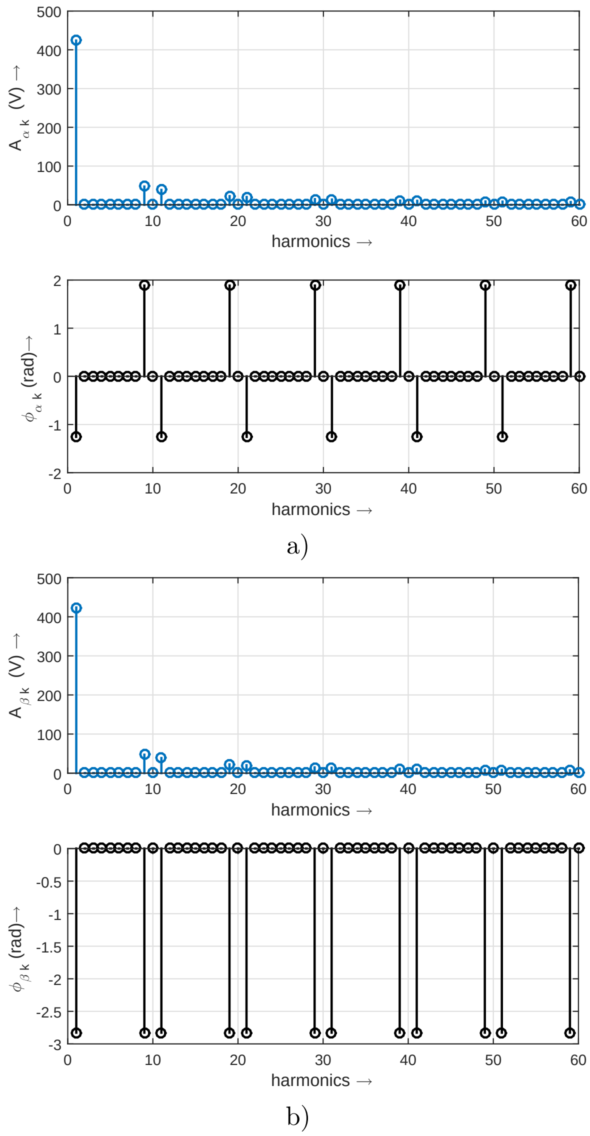

Fig. 7: Harmonic analysis.

the $1, 11, 21, 31, \ldots$ form positive and $9, 19, 29, 39, \ldots$ negative harmonics voltage sequences. There are no zero voltage sequences.

For the harmonic components which form positive voltage sequences, the following relationship is applied:

$$k_p = 1 + 10\,(n-1), \qquad n = 1, 2, 3, \ldots. \tag{9}$$

For negative voltage sequences:

$$k_n = 10\,n - 1, \qquad n = 1, 2, 3, \ldots. \tag{10}$$

3. Motor Currents Calculation

For the stator and rotor current space phasors calculation, a classical equivalent circuit of IM shown in Fig. 8 was used.

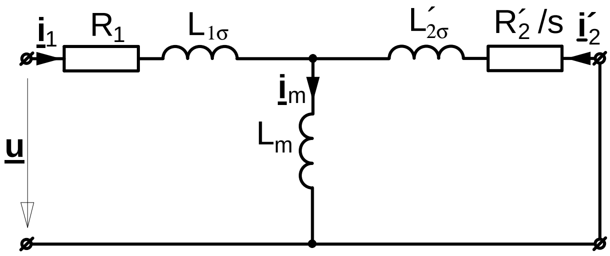

Fig. 8: Equivalent circuit of IM.

The calculation was carried out used measured parameters of five-phase two poles IM. The primed quantities are rated to the effective number of turns of the stator winding (see App. A).

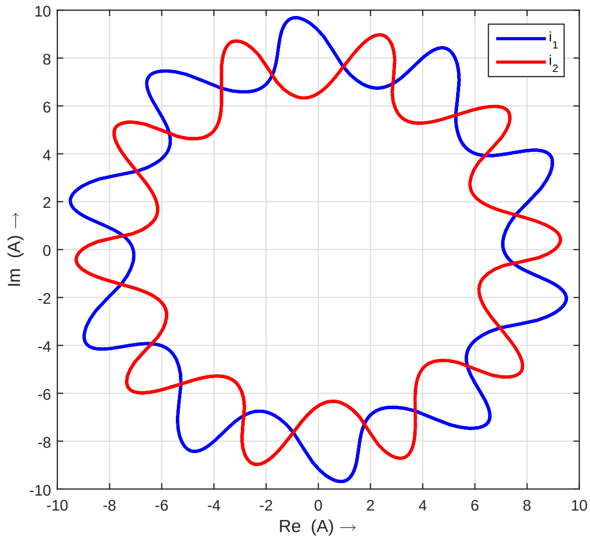

Fig. 9: Stator and rotor current space phasors trajectories.

Referred to the equivalent circuit above, the following equation for the stator current space vector is valid:

$$\begin{bmatrix} \mathbf{u}_k \\ 0 \end{bmatrix} = \begin{bmatrix} R_1 + jX_1 & jX_m \\ jX_m & \dfrac{R_2\prime}{s_k} + jX_2 \end{bmatrix} \begin{bmatrix} \mathbf{i}_{1k} \\ \mathbf{i}_{2k} \end{bmatrix}, \tag{11}$$

where $X_1 = X_{1\sigma} + X_m$, $X_2 = X'_{2\sigma} + X_m$ and $s_k = \frac{k_p\omega - \omega_m}{k_p\omega}$ – slip for the positive, $s_k = 2 - \frac{k_n\omega - \omega_m}{k_n\omega}$ – slip for the negative sequence components. ω_m is the mechanical motor speed.

For the stator and rotor currents components:

$$\begin{bmatrix} \mathbf{i}_{1k} \\ \mathbf{i}_{2k} \end{bmatrix} = \frac{1}{D} \begin{bmatrix} \dfrac{R_2\prime}{s_k} + jX_2 & -jX_m \\ -jX_m & R_1 + jX_1 \end{bmatrix} \begin{bmatrix} \mathbf{u}_k \\ 0 \end{bmatrix}, \tag{12}$$

where, $D = (R_1 + jX_1)\dfrac{R'_2}{s_k} + jR_1X_1 - X_1X_2 + X_m^2$. The sum of current components defines the stator and rotor space phasor:

$$\underline{\mathbf{i}_1} = \sum_{k=1}^{\infty} \mathbf{i}_{1k}, \qquad \underline{\mathbf{i}_2} = \sum_{k=1}^{\infty} \mathbf{i}_{2k}. \tag{13}$$

Calculated stator and rotor current space phasors trajectories are shown in the Fig. 8. The computation was made for nominal motor load and speed (2850 rev·min^{-1}). The motor parameters are listed in App. A.

4. Electromagnetic Torque Calculation

Electromagnetic torque of IM can be determined from the stator or rotor current values according to the formula [18] and [19]:

$$\begin{aligned} M_{em} &= \frac{5}{2}\, p \left(\psi_{1\alpha} i_{1\beta} - \psi_{1\beta} i_{1\alpha}\right) = \\ &= \frac{5}{2}\, p \left(\psi_{2\alpha} i_{2\beta} - \psi_{2\beta} i_{2\alpha}\right). \end{aligned} \tag{14}$$

By using phasors spatial relationship, the Eq (14) comes into the form:

$$M_{em} = \frac{5}{2}\, p\, \mathrm{Im}\left(\underline{\boldsymbol{\psi}}_1^* \underline{\boldsymbol{i}}_1\right) = \frac{5}{2}\, p\, \mathrm{Im}\left(\underline{\boldsymbol{\psi}}_2 \underline{\boldsymbol{i}}_2^*\right). \tag{15}$$

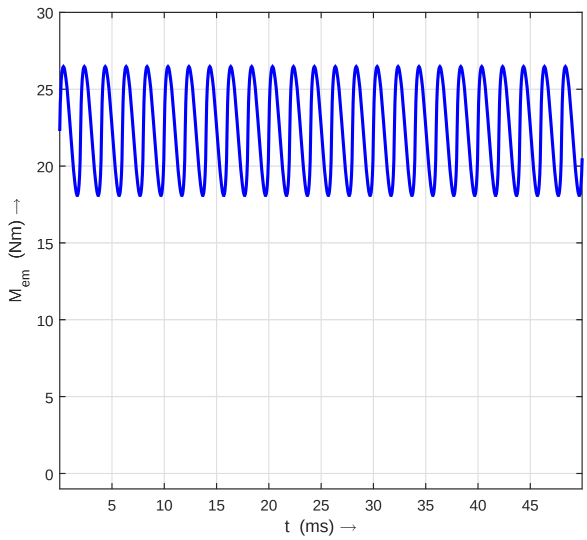

Fig. 10: Electromagnetic torque waveform.

We can express the magnetic flux associated with the stator and rotor in terms of inductance and current. The relationship Eq. (15) changes into the following form: [18]

$$M_{em} = \frac{5}{2}\, p\, L_m\, \mathrm{Im}\left(\underline{\mathbf{i}}_1 \underline{\mathbf{i}}_2^*\right). \tag{16}$$

The calculated time plot of the electromagnetic torque waveform of the five-phase IM pentacle connected and supplied by a rectangular voltage is shown in Fig. 10. The motor is loaded by a nominal load and works at 2850 rev·min^{-1}. In the electromagnetic torque waveform, the fifth harmonic component is well visible. The ripple presents about 20 % of the load torque. Torque magnitude is invariant with load change.

5. Conclusion

The article discusses the electromagnetic torque calculation of the five-phase IM which is pentacle connected. The motor is supplied by a five-phase VSI inverter with rectangular output voltage. Mathematical model using the space phasor theory in the complex plane was build.

In the calculated waveform of electromagnetic torque, a huge five harmonic component is visible. This one stays constant with a change in load. It varies only with the shape of the supply voltage.

Acknowledgment

The financial support of the Slovak Research and Development Agency under the Contract no. APVV-16-0270 is acknowledged.

References

[1] WARD, E. E. and H. Harer. Preliminary investigation of an inverter fed five-phase induction motor. *Proceedings of the Institution of Electrical Engineers*. 1969, vol. 116, iss. 6, pp. 980–984. ISSN 2053-7891. DOI: 10.1049/piee.1969.0182.

[2] KIM, H. M., N. H. KIM and W. S. BAIK. A Five-Phase Induction Motor Speed Control System Excluding Effects of 3rd Current Harmonics Component. *Journal of power electronics*. 2011, vol. 11, iss. 3, pp. 294–303. ISSN 2093-4718. DOI: 10.6113/JPE.2011.11.3.294.

[3] CHOMAT, M., L. SCHREIER and J. BENDL. Effect of stator winding configurations on operation of converter fed five-phase induction machine. In: *International Conference on Electrical Drives and Power Electronics (EDPE)*. Tatranska Lomnica: IEEE, 2015, pp. 21–23. ISBN 978-1-4673-7376-03. DOI: 10.1109/EDPE.2015.7325343.

[4] TRABELSI, M., N. K. NGUYEN and E. SEMAIL. Real-Time Switches Fault Diagnosis Based on Typical Operating Characteristics of Five-Phase Permanent-Magnetic Synchronous Machines. *IEEE Transactions on Industrial Electronics*. 2016, vol. 63, iss. 8, pp. 4683–4694. ISSN 1557-9948. DOI: 10.1109/TIE.2016.2554540.

[5] ESTIMA, J. O. and A. J. M. CARDOSO. A New Algorithm for Real-Time Multiple Open-Circuit Fault Diagnosis in Voltage-Fed PWM Motor Drives by the Reference Current Errors. *IEEE Transactions on Industrial Electronics*. 2013, vol. 60, iss. 8, pp. 3496–3505. ISSN 1557-9948. DOI: 10.1109/TIE.2012.2188877.

[6] SPANIK, P., B. DOBRUCKY, M. FRIVALDSKY, P. DRGONA and I. KURYTNIK. Measurement of swtitching losses in power transistor structure. *Elektronika ir Elektrotechnika*. 2008, vol. 82, no. 2, pp. 75–78. ISSN 1392-1215.

[7] BRANDSTETTER, P., M. KUCHAR and O. SKUTA. Implementation of RBF Neural Network in Vector Control Structure of Induction Motor. *International Review of Electrical Engineering*. 2014, vol. 9, no. 4, pp. 749–756. ISSN 2533-2244. DOI: 10.15866/iree.v9i4.2922.

[8] LEVI, E. Multiphase Electric Machines for Variable-Speed Applications. *IEEE Transactions on Industrial Electronics*. 2008, vol. 55, iss. 5, pp. 1893–1909. ISSN 1557-9948. DOI: 10.1109/TIE.2008.918488.

[9] FRIVALDSKY, M., B. DOBRUCKY, M. PRAZENICA and J. KOSCELNIK. Multi-tank resonant topologies as key design factors for reliability improvement of power converter for power energy applications. *Electrical Engineering*. 2015, vol. 97, iss. 4, pp. 287–302. ISSN 1432-0487. DOI: 10.1007/s00202-015-0336-3.

[10] FRIVALDSKY, M., B. DOBRUCKY and M. PRIDALA. Analysis of LCLC DC-DC resonant converter in steady state operation. In: *42nd Annual Conference of the IEEE Industrial Electronics Society*. Florence: IEEE, 2016, pp. 24–27. ISBN 978-1-5090-3474-1. DOI: 10.1109/IECON.2016.7793216.

[11] ZASKALICKY, P. Mathematical model of a five-phase voltage-source PWM-controlled inverter. *Electrical Engineering*. 2017, vol. 99, iss. 4, pp. 1179–1184. ISSN 1432-0487. DOI: 10.1007/s00202-017-0643-y.

[12] ZASKALICKA, M., P. ZASKALICKY, M. BENOVA, M.A.R. ABDALMULA, B. DOBRUCKY. Analysis of complex time function of converter

output quantities using complex fourier transform/series. *Communications - Scientific Letters of the University of Zilina*. 2010, vol. 12, no. 1, pp. 23–30. ISSN 2585-7878.

[13] DOBRUCKY, B., O. V. CERNOYAROV and M. MARCOKOVA. Computation of the total harmonic distortion of impulse system quantities using infinite series. In: *Proceedings of 14th Conference on Applied Mathematics (APLIMAT 2015)*. Bratislava: Slovak University of Technology in Bratislava, 2015, pp. 213–220. ISBN 978-1-510-80123-3.

[14] DOBRUCKY, B., M. MARCOKOVA and P. STEFANEC. Analytic Solution of the Multi-Resonant Electrical Circuit under Impulse Supply. In: *16th Conference on Applied Mathematics (APLIMAT 2017)*. Bratislava: Slovak University of Technology in Bratislava, 2017, pp. 467–472. ISBN 978-1-5108-3698-3.

[15] ZHAO, P. and T. A. LIPO. Space vector PWM control of dual three-phase induction machine using vector space decomposition. *IEEE Transactions on Industry Applications*. 1995, vol. 31, iss. 5, pp. 1100–1109. ISSN 1939-9367. DOI: 10.1109/28.464525.

[16] IQBAL, A. and E. LEVI. Space Vector PWM Techniques for Sinusoidal Output Voltage Generation with Five-Phase Voltage Source Inverter. *Electric Power Components and Systems*. 2006, vol. 34, iss. 2, pp. 119–140. ISSN 1532-5008. DOI: 10.1080/15325000500244427.

[17] RYU, H.-M., J.-H. KIM and S.-K. SUL. Analysis of Multiphase Space Vector Pulse-Width Modulation Based on Multiple d–q Spaces Concept. *IEEE Transactions on Power Electronics*. 2005, vol. 20, iss. 6, pp. 1364–1371. ISSN 1941-0107. DOI: 10.1109/TPEL.2005.857551.

[18] CHATELAIN, J. *Machines electriques*. 1st ed. Paris: Dunod, 1983, ISBN 978-2-04-015620-6.

[19] CHAPMAN, S. J. *Electric machinery fundamentals*. 4th ed. New York: Mc-Graw-Hill, 2005, ISBN 978-0-07-246523-5.

About Authors

Pavel ZASKALICKY was born in Liptovsky Mikulas (1949), Slovak Republic. He works on the Department of Electrical Engineering and Mechatronics, Faculty of Electrical Engineering and Informatics (FEI) of the Technical University (TU) in Kosice. After graduating from the Faculty of Electrical Engineering of the University of Technology in Kosice (1975) he started to work in Energoprojekt Praha as a designer. Since 1977 he worked as an assistant, later as a lecturer at the Department of Electrical Drives at Faculty of Electrical Engineering of the Technical University of Kosice. In 1985 he received his Ph.D. degree. In 1989 he left for the Universite Technique de Sidi-Bel Abbes, Algeria, where he worked until 1991. In 1991–1995 he worked at Ecole National Superieur d'Electricite et de Mecanique (ENSEM), National Polytechnic Institute of Lorraine (INPL) Nancy France where he was involved both in education and research. He co-authored the general theory of asymmetric reluctance motors.

In 1995 he returned to FEI TU Kosice, where he became Associate Professor in 1997, and in 2007 Full Professor.

Prof. Zaskalicky works in the field of mathematical simulations of electrical machines and power electronic converters. He deals with influence of non-harmonic supply on properties of electrical machines and also with modeling of semiconductor converters using complex Fourier series. He was a successful principal investigator of several research Science Grand Agency (VEGA) and Slovak Research and Development Agency (APVV) projects in Slovak Republic. He is a member of committees of several international conferences and scientific technical journals.

Appendix A
AC Drive Parameters

$P_n = 6.5$ kW; $U_n = 5 \times 230$ V/50 Hz;
$n_n = 2850$ rev·min^{-1}; $p = 1$;
$R_1 = 3.778\ \Omega$; $R_2' = 2.498\ \Omega$;
$L_m = 0.436$ H; $L_{1\sigma} = 6.83$ mH; $L_{2\sigma}' = 11.88$ mH;